PHYSICAL REVIEW A VOLUME 49, NUMBER 3 MARCH 1994

Hydrogen molecule under confinement: Exact results

Tao Pang
Department of Physics, University of Nevada, Las Vegas, Nevada 89154-4002

(Received 8 October 1993)

The properties of a hydrogen molecule under spatial confinement are studied by diffusion quantum Monte Carlo simulations. The ground-state energy and the bond length of the molecule are evaluated under an equilibrium spheroidal-box condition. Since the calculations of the ground-state properties for this specific system are exact from the diffusion quantum Monte Carlo simulations, the results obtained here can also serve as a criterion to any approximate or variational method applied to highly correlated electronic systems. The possibility of further work to calculate the vibrational frequency and other pressure-dependent physical quantities is discussed.

PACS number(s): 31.20.−d, 36.20.Hb, 02.70.Lq

I. INTRODUCTION

There has been a great deal of interest in the properties of hydrogen molecules under high pressure [1–3]. For example, the metal-insulator transitions [1,2,4,5] and the structural phase transitions [6,7] of hydrogen solids above 100 GPa. Recently there have been experimental studies on the properties of hydrogen molecules confined in neon, helium, and argon matrices under high pressure [8]. It is noted that the pressure dependence of the bond length and the pressure dependence of the vibrational frequency of the molecule under the high pressure [8] are similar to those calculated from a variational approach [9] of a hydrogen molecule confined in a spheroidal box under equilibrium condition.

When a hydrogen molecule is located inside a matrix, for example, in a neon matrix, it behaves qualitatively the same as it is confined inside a cavity. A significant question is how sensitive the properties, such as the molecular energy, bond length, and vibrational frequency, are to the shape of the cavity. Since the previous calculations are all variational, it is impossible to determine the quantitative difference between the experimental measurements and a simple model such as a spheroidal box.

In this work, we present calculations of the properties of a hydrogen molecule in an equilibrium spheroidal box from diffusion quantum Monte Carlo simulations. The equilibrium here means that the bond length and the minor axis of the box are adjusted to optimize the ground-state energy of the molecule for a given major axis. The calculations here are exact and the only errors are from the statistics and the finite time step of the simulation. And both of them can be controlled to be as small as desired. This work is the first part of a planned project to calculate all physical properties of a hydrogen molecule confined in a spheroidal box by quantum Monte Carlo simulations, including the pressure dependence of the vibrational frequency and bond length and the sensitivity of these quantities to the shape of the box. We will present here the calculations of the molecular energy and the equilibrium bond length of a hydrogen molecule in a spheroidal box with a given major axis. The molecule is assumed to have two protons located at the foci of the spheroidal box. So the equilibrium is achieved by searching for a proper bond length, or minor axis, to optimize the total ground-state energy of the system.

II. HAMILTONIAN

For a hydrogen molecule inside a spheroidal box defined by

$$\frac{x^2}{b^2} + \frac{y^2}{b^2} + \frac{z^2}{a^2} = 1, \tag{2.1}$$

the Hamiltonian of the system is given by

$$H = H(1) + H(2) + \frac{1}{r_{12}} + \frac{1}{R_{ab}}, \tag{2.2}$$

with

$$H(i) = -\frac{1}{2}\nabla_i^2 - \frac{1}{r_{ia}} - \frac{1}{r_{ia}}, \tag{2.3}$$

where the protons are put at the foci of the box along the z axis. a is the semimajor axis. r_{ia} and r_{ib} are the distances between the ith electron and two protons, and r_{12} is the distance between two electrons. R_{ab} is the separation of two protons. Now if we assume that two protons are located at the foci of the spheroidal box at the equilibrium, we have $R_{ab}^2 = 4(a^2 - b^2)$, with b the semiminor axis. So for a given a, one can adjust R_{ab} (adjustment on b will follow) to search for the ground state of the system by optimizing the molecular energy.

If we apply the Born-Oppenheimer approximation to the system, we can treat the proton wave function and electron wave function separately, that is, solve the electron wave equation for a given proton configuration. The molecular energy is then given by

$$E_m = E_0 + \frac{1}{R_{ab}}, \tag{2.4}$$

where E_0 is the ground-state energy of electrons of Eq. (2.2) for a given separation of two protons R_{ab}.

1050-2947/94/49(3)/1709(5)/$06.00

Atomic units (a.u.) are used throughout this article. The energy is in hartrees and the length is in the Bohr radius, which corresponds to setting $m_e = e = \hbar = c = 1$.

III. THE QUANTUM MONTE CARLO METHOD

In order to obtain the exact ground-state energy of Eq. (2.2), a diffusion quantum Monte Carlo method (DQMC) is employed to simulate the Schrödinger equation as a diffusion equation of a time-dependent probability in configuration space [10,11].

In the DQMC approach for an N-electron system, one takes a variational wave function $\Phi(\mathbf{R})$ with $\mathbf{R} = (\mathbf{r}_1, \mathbf{r}_2, ..., \mathbf{r}_N)$ as a guiding wavefunction for the ground state and then constructs a time-dependent probability density $F(\mathbf{R}, t)$ from

$$F(\mathbf{R}, t) = \Psi(\mathbf{R}, t)\Phi(\mathbf{R}), \tag{3.1}$$

with

$$\Psi(\mathbf{R}, t) = \exp\left(\int_0^t E_n(t')dt' - Ht\right)\Phi(\mathbf{R}), \tag{3.2}$$

where $E_n(t)$ is an adjustable constant which can be considered as a normalization factor at the moment. If one writes the Schrödinger equation in an imaginary time form and multiples the equation by the guiding wave function, one has

$$\frac{\partial F}{\partial t} = \frac{1}{2}\nabla^2 F - \nabla \cdot F\mathbf{U} - [E_n - E(\mathbf{R})]F, \tag{3.3}$$

with $\mathbf{U}$ as a drifting velocity $\mathbf{U} = \nabla \ln \Phi(\mathbf{R})$ and $E(\mathbf{R}) = \Phi^{-1}(\mathbf{R})H\Phi(\mathbf{R})$ as a local energy of a given configuration $\mathbf{R}$. As long as $\Phi(\mathbf{R})$ is not orthogonal to the exact ground state of H, $\Psi(\mathbf{R}, t)$ will approach the true ground state of H when t goes to infinity. If one defines a time-dependent expectation value $E(t)$

$$E(t) = \frac{\langle\Phi(\mathbf{R})|H|\Psi(\mathbf{R}, t)\rangle}{\langle\Phi(\mathbf{R})|\Psi(\mathbf{R}, t)\rangle} = \frac{\int d\mathbf{R}F(\mathbf{R}, t)E(\mathbf{R})}{\int d\mathbf{R}F(\mathbf{R}, t)}, \tag{3.4}$$

which becomes the exact ground-state energy of H as t goes to infinity. What one has to do now is to simulate the configuration $\mathbf{R}$ according to the distribution function F($\mathbf{R}$,t) and then let the time evolve to a target time where the dominant error is from statistics.

In practice, the simulation is done by rewriting the diffusion equation for $F(\mathbf{R}, t)$ into an integral form:

$$F(\mathbf{R}', t + \tau) = \int d\mathbf{R}F(\mathbf{R}, t)G(\mathbf{R}', \mathbf{R}; \tau), \tag{3.5}$$

where $G(\mathbf{R}', \mathbf{R}; \tau)$ is the Green's function of Eq. (3.3). If τ is very small, the Green's function can be approximated as

$$G(\mathbf{R}', \mathbf{R}; \tau) \simeq W(\mathbf{R}', \mathbf{R}; \tau)G_0(\mathbf{R}', \mathbf{R}; \tau), \tag{3.6}$$

where

$$G_0(\mathbf{R}', \mathbf{R}; \tau) = \left(\frac{1}{2\pi\tau}\right)^{3N/2} e^{-[\mathbf{R}'-\mathbf{R}-\mathbf{U}\tau]^2/2\tau} \tag{3.7}$$

is a propagator with a drifting velocity $\mathbf{U}$ and

$$W(\mathbf{R}', \mathbf{R}; \tau) = e^{-\{[E(\mathbf{R})+E(\mathbf{R}')]/2-E_n(t)\}\tau} \tag{3.8}$$

is a branching factor. So the actual simulations are done as follows.

(1) First one generates an ensemble of configurations according to F($\mathbf{R}$,0) from the guiding wave function. The parameters in the guiding wave function are optimized through variational Monte Carlo simulations.

(2) Then each configuration is moved by a drifting term and a Gaussian random step $\mathbf{R}' = \mathbf{R} + \mathbf{U}\tau + \chi$, where χ is a $3N$-dimensional Gaussian random number with a variance of τ on each component.

(3) The move is accepted with a probability $\min[1, A(\mathbf{R}', \mathbf{R}; \tau)]$, with

$$A(\mathbf{R}', \mathbf{R}, \tau) = \frac{\Phi(\mathbf{R}')^2 G(\mathbf{R}, \mathbf{R}'; \tau)}{\Phi(\mathbf{R})^2 G(\mathbf{R}', \mathbf{R}; \tau)}, \tag{3.9}$$

to ensure detailed balance. When the guiding wave function has a nodal structure, we use the fixed node approximation which eliminates the configurations with attempted moves across a node. This fixed node approximation still gives the upper bound energy and can be released if needed [12].

(4) The new ensemble is created from branching by placing $M = [W(\mathbf{R}', \mathbf{R}; \tau_a) + \xi]$ copies of the the configuration $\mathbf{R}'$ into the new ensemble, where ξ is a uniform random number between [0,1] and τ_a is the effective diffusion time which is proportional to τ with a coefficient as the ratio of mean square distance accepted to the mean square distance attempted from a simple argument of random diffusion. Since we treat the whole configuration as one point in the configuration space and all the coordinates in that configuration are either updated at the same time or kept unchanged after attempted move, the effective diffusion time τ_a then is either equal to τ for the configuration which is moved or zero for the configuration which is unchanged. In practice, one can simply choose $\tau_a = \tau$ if τ is small enough since the equilibrium configurations will have an approximate acceptance probability of 1.

The average local energy $\bar{E}(\mathbf{R}')$ is then calculated from $E(\mathbf{R}')$ weighted by $W(\mathbf{R}', \mathbf{R}; \tau)$ in the whole ensemble. The parameter $E_n(t)$ is then adjusted to $[\bar{E}(\mathbf{R}) + \bar{E}(\mathbf{R}')]/2$.

Repeat the above steps to a target time when the error is dominated by statistics; then start taking data for calculations with a frequency which is determined from the autocorrelation function of the quantity evaluated. Group the data and average them to the desired accuracy. Several independent runs should be carried out to ensure that the averaged data is free from an accidental fluctuation. The ensemble can be also saved for the longer runs to generate more blocks of data.

IV. THE GUIDING WAVE FUNCTION

In this work, we choose a simple singlet wave function for the two electrons in the system as the guiding wave function:

$$\Phi(\mathbf{R}) = f(r_{12})g(\mathbf{r}_1)g(\mathbf{r}_2), \tag{4.1}$$

where $f(r)$ is the two-body Jastrow correlation factor

$$f(r) = \exp\left[\frac{r}{2(1+\beta r)}\right], \tag{4.2}$$

with β as an as yet undetermined variational parameter. $g(\mathbf{r}_i)$ is a single-particle wave function given by

$$g(\mathbf{r}) = [e^{-\alpha r_a} + e^{-\alpha r_b}][\lambda(\mathbf{r}) - 1], \tag{4.3}$$

with

$$\lambda(\mathbf{r}) = \frac{x^2}{b^2} + \frac{y^2}{b^2} + \frac{z^2}{a^2}. \tag{4.4}$$

Here α is determined from $\alpha = 1/[1 + \exp(-R_{ab}/\alpha)]$ to fulfill the cusp condition for an electron moving in the field of two protons separated by a distance R_{ab}. Then β is the only variational parameter left in the guiding wave function. The parameter β for a given setup is then determined variationally by doing a variational Monte Carlo simulation first and then the wave function is used as a guide to carry out the diffusion Monte Carlo simulations described in Sec. III. The wave function outside of the spheroidal box is set to zero, of course. The cusp conditions fulfilled by the Jastrow correlation factor and the single-particle wave function are extremely important in inhibiting the numerical fluctuations during the simulation.

Here we show some parameters used in the simulations in this work. As one can see from the data in Table I, the variational parameter β in the guiding wave function increases approximately linearly with the decrease of a and the random walk step Δr decreases approximately linearly with the decease of a in order to have about a 50% acceptance rate in the random walks of the variational quantum Monte Carlo simulations. This is expected because the semimajor axis a determines the length scale of the system and both β and Δr reflect that length scale. A smaller time step is taken for the case of $a = 1$ because of the strong confinement there and the step of each attempted move has to be small in order to keep the system stable in the initial runs.

TABLE I. The parameters used in the calculations. Δt is the time step used, Δr is the space step used in the variational calculation to set up the configurations, and β is the variational parameter used for the given semimajor axis a. All quantities are given in atomic units.

a	Δt	Δr	β
∞	0.0010	1.90	0.11
5	0.0010	1.50	0.13
4	0.0010	1.35	0.14
3	0.0010	1.15	0.15
2	0.0010	0.90	0.16
1	0.0002	0.70	0.18

V. SIMULATION RESULTS

We have performed diffusion quantum Monte Carlo simulations on RISC/6000 computer workstations and on a Cray-YMP supercomputer for a hydrogen molecule confined in a spheroidal box. We have calculated the ground-state energy of a molecule in a spheroidal box with a fixed semimajor axis. The equilibrium bond length and minor axis of the spheroidal box are searched by optimizing the ground-state energy of the molecular system. In Table II, we show the optimized ground-state energy and the optimized bond length with a given semimajor axis. The variational calculations [9] done on the same systems are also listed for comparison. As one can see from the table, the variational calculations on both energy and bond length are quite accurate.

We also plot the results of the molecular energy of a hydrogen molecule in a spheroidal box in Fig. 1. Clearly the trend of the molecular energy versus the inverse of the semimajor axis of the spheroidal box, the measure of the confinement, is well described by the variational calculations of LeSar and Herschbach [9]. This is an indication that the calculations on the pressure dependence of the bond length and vibrational frequency from the variational method [9] may have given a good description of the system. The variational calculations of the pressure dependence of the vibrational frequency and the equilibrium bond length of a hydrogen molecule [9] is, in fact, in qualitative agreement with the recent experimental measurements of the pressure dependence of the vibrational frequency and bond length of hydrogen molecules in neon and other matrices under high pressure [8].

We search the equilibrium bond length and semiminor axis by optimizing the molecular energy as follows. First we use variational Monte Carlo simulations to determine the parameters in the guiding wave function and estimate roughly the equilibrium bond length. Then we use diffusion quantum Monte Carlo simulations to obtain three sets of data around the points determined in the variational Monte Carlo simulations. With the three sets of data for different bond lengths and energies, we assume that they fulfill a quadratic curve

$$E_m^i = E_m + \alpha(R_{ab}^i - R_{ab})^2 \tag{5.1}$$

TABLE II. The comparison of ground-state energies and optimized bond length for a given semimajor axis. R_{ab}^v and E_m^v are the variational calculations of LeSar and Herschbach [9] and R_{ab} and E_m are the results of the DQMC calculations of the present work. All quantities are given in atomic units.

a	R_{ab}^v	E_m^v	R_{ab}	E_m
∞	1.403	-1.1716	1.4010	-1.1746(5)
5	1.395	-1.1638	1.3895	-1.1702(3)
4	1.355	-1.1440	1.3503	-1.1533(5)
3	1.208	-1.0441	1.1771	-1.0523(9)
2	0.893	-0.4749	0.8949	-0.4790(10)
1	0.455	4.5947	0.4493	4.5944(30)

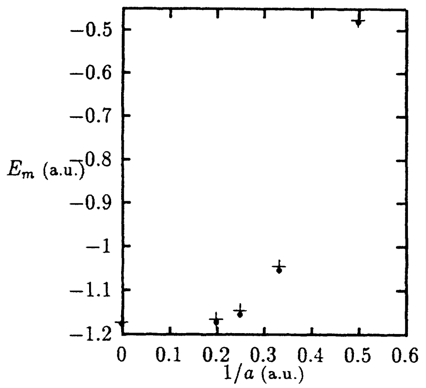

FIG. 1. The plot shows the optimized ground-state energy versus the inverse of the semimajor axis of the spheroidal box. The crosses are variational results of LeSar and Herschbach [9] and the dots are the quantum Monte Carlo simulation results of the present work.

with E_m, α, and R_{ab} to be solved from three sets of E^i_m and R^i_{ab}. The data shown in Table II are the optimized energy E_m and the equilibrium bond length R_{ab} in Eq. (5.1). In Table III, the data E^i_m and R^i_{ab} for each given semimajor axis obtained from the simulations are shown.

VI. CONCLUSIONS

In this work, we have calculated the equilibrium ground-state energy and bond length of a hydrogen molecule confined in a spheroidal box with a given semimajor axis. Most of the exact molecular energies that we have obtained are about 1% lower than those of the variational calculations done by LeSar and Herschbach [9]. Most of the equilibrium bond lengths that we have obtained are shorter than those calculated from the variational method for a given semimajor axis. The trend of the molecular energy as shown in Fig. 1 are in good agreement with the variational calculations. For this system, the diffusion quantum Monte Carlo can in principle give exact results within the statistical errors and therefore are useful to check any variational methods developed for electronic systems.

One important aspect which is still under investigation is how well this model describes the behavior of hydrogen molecules in an actual matrix under high pressure, such as hydrogen molecules in a neon matrix [8]. Experimentally, the vibrational frequency is increased and the bond length is decreased with the increase of the pressure.

TABLE III. The ground-state energies and corresponding bond lengths for a given semimajor axis calculated from the diffusion quantum Monte Carlo simulations. All quantities are given in atomic units.

a	R^1_{ab}	E^1_m	R^2_{ab}	E^2_m	R^3_{ab}	E^3_m
5	1.395	-1.1698	1.390	-1.1702	1.385	-1.1699
4	1.355	-1.1522	1.350	-1.1533	1.345	-1.1515
3	1.200	-1.0497	1.195	-1.0507	1.190	-1.0515
2	0.900	-0.4745	0.895	-0.4790	0.890	-0.4749
1	0.455	4.5974	0.450	4.5945	0.445	4.5962

There has been a recent quantum Monte Carlo simulation study on the properties of two-electron atomic system under a spherical confinement [13]. The calculations on the ground-state energy versus the radius of the sphere in Ref. [13] have some similar features of the ground-state energy which we have obtained for the hydrogen molecule here versus the semimajor axis of the spheroidal box. Electronic systems under confinement have shown some other interesting phenomena too. The most noticeable are the structural phase transitions observed experimentally in solid hydrogen [6,7] and solid helium [14] and the metal-insulator transitions in solid hydrogen under high pressure [1,2]. A diffusion quantum Monte Carlo simulation study was carried out for the solid hydrogen system [3] and this has been the most impressive work of quantum Monte Carlo simulations to date. It is our hope that further development of the quantum Monte Carlo simulation will allow its use to study larger and more complicated systems, especially clusters and solids under high pressure. This includes the development of the Monte Carlo simulations on parallel and distributed computer environments.

Quantum Monte Carlo simulations [15] have penetrated into many areas of physics and chemistry now. Recent examples include studies of the vibrational states of molecules and clusters [16] and the barrier height in the reaction H + H_2 → H_2 + H [17]. Another important development in the past few years is the implementation of the quantum Monte Carlo simulations to a parallel computer [18]. The aspect of doing quantum Monte Carlo simulations on distributed and parallel computers will be explored in future work on this project.

ACKNOWLEDGMENTS

This work was supported in part by the National Supercomputer Center for Energy and the Environment at the University of Nevada, Las Vegas (UNLV), the University Fellowships and Grants Committee of UNLV, the Army High Performance Computer Research Center at the University of Minnesota, and IBM.

APPENDIX: ADOPTED RANDOM-NUMBER GENERATOR

In this work, we have used a linear congruential method to generate the random numbers needed for the simulations. The sequence of the random numbers in this method is

$$x_{i+1} = (ax_i + b) \bmod c. \tag{A1}$$

We have chosen $a = 7^7 = 16\,807$, $b = 0$, and $c = 2^{31} - 1 = 2\,147\,483\,647$ as suggested by the minimum standards for good random-number generators [19]. It was also shown in a recent Monte Carlo simulation study [20] of liquid helium with several random-number generators that the random-number generator which we have adopted is a good one. To implement this random-number generator on any machine with 32 bits or more, one can use the following algorithm:

$$x_{i+1} = \begin{cases} a \bmod (x_i, q) - r \operatorname{int} (x_i/q), & \text{if } x_{i+1} > 0 \\ c + a \bmod (x_i, q) - r \operatorname{int} (x_i/q) & \text{otherwise,} \end{cases} \tag{A2}$$

where $q = \operatorname{int}(c/a)$ and $r = \operatorname{mod}(c, a)$. In the main program, in order to start the program every time with a different seed, one can use the time statement from the c library on the UNIX systems, or Cray time on the Cray computers.

[1] H. K. Mao and R. J. Hemley, Science **244**, 1462 (1989); **247**, 864 (1990); R. J. Hemley and H. K. Mao, *ibid.* **249**, 391 (1990).

[2] I. F. Silvera, Science **247**, 863 (1990).

[3] D. M. Ceperley and B. J. Alder, Phys. Rev. B **36**, 2092 (1987).

[4] H. Chacham and S. G. Louie, Phys. Rev. Lett. **66**, 64 (1991).

[5] M. P. Surh, T. W. Barbee III, and C. Mailhiot, Phys. Rev. Lett. **70**, 4090 (1993).

[6] H. E. Lorenzana, I. F. Silvera, and K. A. Goettel, Phys. Rev. Lett. **64**, 1939 (1990).

[7] K. J. Runge, M. P. Surh, C. Mailhiot, and E. L. Pollock, Phys. Rev. Lett. **69**, 1939 (1992); **70**, 2974(E) (1993).

[8] P. Loubeyre, R. Letoullec, and J. P. Pinceaux, Phys. Rev. Lett. **67**, 3271 (1991); Phys. Rev. B **45**, 12 844 (1992).

[9] R. LeSar and D. R. Herschbach, J. Chem. Phys. **85**, 2798 (1981).

[10] P. J. Reynolds, D. M. Ceperley, B. J. Alder, and W. A. Lester, Jr., J. Chem. Phys. **77**, 5593 (1982).

[11] W. A. Lester, Jr. and B. L. Hammond, Annu. Rev. Phys. Chem. **41**, 283 (1990).

[12] D. M. Ceperley and B. J. Alder, J. Chem. Phys. **81**, 5833 (1984).

[13] C. Joslin and S. Goldman, J. Phys. B **25**, 1965 (1992).

[14] P. Loubeyre, R. LeToullec, J. C. Pinceaux, H. K. Mao, J. Hu, and R. J. Hemley, Phys. Rev. Lett. **71**, 2272 (1993).

[15] D. M. Ceperley and B. J. Alder, Science **231**, 555 (1986).

[16] M. A. Suhm and R. O. Watts, Phys. Rep. **204**, 293 (1991).

[17] D. L. Diedrich and J. B. Anderson, Science **258**, 786 (1992).

[18] C. A. Traynor, J. B. Anderson, and B. M. Boghosian, J. Chem. Phys. **94**, 3657 (1991).

[19] S. K. Park and K. W. Miller, Commun. ACM **31**, 1192 (1988).

[20] A. M. Ferrenburg, D. P. Landau, and Y. J. Wong, Phys. Rev. Lett. **69**, 3382 (1992).